OXFORD

Cerebral Cortex, 2022, **32**, 5108–5120
https://doi.org/10.1093/cercor/bhac001
Advance access publication date 24 January 2022
Original Article

Co-expression network analysis of frontal cortex during the progression of Alzheimer's disease

John S. Beck[1], Zachary Madaj[2], Calvin T. Cheema[3], Betul Kara[1,4], David A. Bennett[5,6], Julie A. Schneider[5,6], Marcia N. Gordon[1], Stephen D. Ginsberg[7,8,9,10], Elliott J. Mufson[11], Scott E. Counts[1,4,12,13,14,*]

[1]Department of Translational Neuroscience, Michigan State University, Grand Rapids, MI 49503, USA,
[2]Bioinformatics and Biostatistics Core, Van Andel Research Institute, Grand Rapids, MI 49503, USA,
[3]Department of Mathematics and Computer Science, Kalamazoo College, Kalamazoo, MI 49006, USA,
[4]Cell and Molecular Biology Program, Michigan State University, East Lansing, MI 48824, USA,
[5]Department of Neurological Sciences, Rush University Medical Center, Chicago, IL 60612, USA,
[6]Rush Alzheimer's Disease Research Center, Chicago, IL 60612, USA,
[7]Center for Dementia Research, Nathan Kline Institute, Orangeburg, NY 10962, USA,
[8]Department of Psychiatry, New York University Grossman School of Medicine, New York, NY 10016, USA,
[9]Department of Neuroscience and Physiology, New York University Grossman School of Medicine, New York, NY 10016, USA,
[10]NYU Neuroscience Institute, New York University Grossman School of Medicine, New York, NY 10016, USA,
[11]Department of Neurobiology, Barrow Neurological Institute, Phoenix, AZ 85013, USA,
[12]Department of Family Medicine, Michigan State University, Grand Rapids, MI 49503, USA,
[13]Hauenstein Neurosciences Center, Mercy Health Saint Mary's Hospital, Grand Rapids, MI 49503, USA,
[14]Michigan Alzheimer's Disease Research Center, Ann Arbor, MI 48109, USA
*Address correspondence to Scott E. Counts, 400 Monroe Avenue NW, Grand Rapids, MI 49503, USA. Email: countssc@msu.edu

Mechanisms of Alzheimer's disease (AD) and its putative prodromal stage, amnestic mild cognitive impairment (aMCI), involve the dysregulation of multiple candidate molecular pathways that drive selective cellular vulnerability in cognitive brain regions. However, the spatiotemporal overlap of markers for pathway dysregulation in different brain regions and cell types presents a challenge for pinpointing causal versus epiphenomenal changes characterizing disease progression. To approach this problem, we performed Weighted Gene Co-expression Network Analysis and STRING interactome analysis of gene expression patterns quantified in frontal cortex samples (Brodmann area 10) from subjects who died with a clinical diagnosis of no cognitive impairment, aMCI, or mild/moderate AD. Frontal cortex was chosen due to the relatively protracted involvement of this region in AD, which might reveal pathways associated with disease onset. A co-expressed network correlating with clinical diagnosis was functionally associated with insulin signaling, with insulin (*INS*) being the most highly connected gene within the network. Co-expressed networks correlating with neuropathological diagnostic criteria (e.g., NIA-Reagan Likelihood of AD) were associated with platelet-endothelium-leucocyte cell adhesion pathways and hypoxia-oxidative stress. Dysregulation of these functional pathways may represent incipient alterations impacting disease progression and the clinical presentation of aMCI and AD.

Key words: amnestic mild cognitive impairment; cell cycle; endothelium; insulin signaling; oxidative stress.

Introduction

Alzheimer's disease (AD) results in a significant departure from the trajectory of normal cognitive aging and is the most common cause of dementia. Diagnostic criteria of AD include the presence of extracellular senile plaques, which are fibrillar aggregates of amyloid-β (Aβ) peptides often embedded with dystrophic neurites, and intracellular neurofibrillary tangles (NFTs) containing aggregates of hyperphosphorylated, misfolded moieties of the protein tau (Hyman et al. 2012; Jack Jr et al. 2016). The mechanisms underlying the pathobiology of AD remain elusive as the vast majority of cases are sporadic, arising from an unknown combination of genetic and environmental factors (Mufson, Ikonomovic, et al. 2016; Jack Jr et al. 2018). This lack of clarity on disease etiology is compounded by preclinical and prodromal stages that may span decades on a heterogenous background of individual reserve, resistance, and resilience (Montine et al. 2019). With respect to the potential molecular and cellular differences underlying disease heterogeneity, we and others have shown in cross-sectional postmortem tissue studies that the progression of AD is characterized by the dysregulation of multiple gene families in corticopetal and corticocortical projection neurons regulating cognitive function (Dunckley et al. 2006; Ginsberg et al. 2006; Counts et al. 2013; Kelly et al. 2017). However, the spatiotemporal overlap of these gene expression changes in different brain regions and cell types presents a challenge for pinpointing causal versus epiphenomenal pathway alterations during disease progression.

Received: October 21, 2021. **Revised:** December 20, 2021. **Accepted:** December 21, 2021

As bioinformatic inquiry has developed along with expression profiling strategies, Weighted Gene Co-expression Network Analysis (WGCNA) offers an attractive option for examining multifactorial disease presentations to meet this challenge (Miller et al. 2013; Seyfried et al. 2017; Alldred et al. 2021). This integrated systems biology approach allows for the unbiased interrogation of gene expression datasets to cluster genes into modules exhibiting correlated levels of expression. Highly correlated genes within discrete modules can then be examined for overrepresentation within specific endophenotypes and functional pathways. To this end, we analyzed gene expression patterns across the AD spectrum via microarray analysis of frozen frontal cortex samples (Brodmann area [BA] 10) from subjects who died with a clinical diagnosis of no cognitive impairment (NCI), amnestic mild cognitive impairment (aMCI, a putative prodromal AD stage), or mild/moderate AD. Frontal cortex was chosen for analysis given the relatively protracted involvement of this region in AD pathogenesis, which might reveal functional pathways associated with incipient pathological changes. Alternatively, given several lines of evidence that frontal cortex undergoes neuroplastic remodeling in the face of mounting pathology during MCI (DeKosky et al. 2002; Counts et al. 2006; Bell et al. 2007; Williams et al. 2009; Bossers et al. 2010; Weinberg et al. 2015), analysis of this region might also help reveal pathways mediating resilience. These expression patterns may likewise influence the role of frontal cortex as a functional hub of resting state networks such as the default mode network (Liu et al. 2013; Moayedi et al. 2015; DeSerisy et al. 2021), which mediates memory and attentional functions and falters in AD (Simic et al. 2014; Dillen et al. 2017). Hence, the identified networks and their molecular components may provide new clues to disease-modifying therapeutic targets for AD.

Materials and Methods

Subjects

Postmortem tissue samples were obtained from participants in the Rush Religious Order Study (RROS), a longitudinal clinical pathologic study of aging and dementia in elderly Catholic clergy members. Details of RROS clinical and neuropathologic evaluations and diagnostic criteria are published (Bennett et al. 2002; Counts et al. 2006; Schneider et al. 2009). Briefly, RROS participants undergo an annual neurological examination and cognitive performance testing using the Mini-Mental State Exam (MMSE) and 19 additional neuropsychological tests referable to five cognitive domains: orientation, attention, memory, language, and perception (Bennett et al. 2002). A Global Cognitive Score (GCS) consisting of a composite z-score calculated from this test battery is then determined for each participant (Bennett et al. 2002). The diagnosis of dementia due to AD follows the revised recommendations from the National Institute on Aging-Alzheimer's Association workgroups on diagnostic guidelines for AD (McKhann et al. 2011). The aMCI population is defined as subjects who exhibited impairment in episodic memory—and possibly other cognitive domains—but did not meet the criteria for AD or dementia, which is consistent with criteria used by others in the field (Morris et al. 2001; Petersen 2004; Abner et al. 2012). Cases with clinically and/or neuropathologically diagnosed comorbidities, such as large strokes, parkinsonism, Lewy body dementia, frontotemporal dementia, hippocampal sclerosis, or major depressive disorder, were excluded from the study.

A board-certified neuropathologist evaluated all cases while blinded to clinical diagnosis (Schneider et al. 2009). Designations of "normal" (with respect to AD or other dementing processes), "possible AD," "probable AD," or "definite AD" were based on semi-quantitative estimation of neuritic plaque density, an age-related plaque score, and presence or absence of dementia as established by the Consortium to Establish a Registry for Alzheimer's Disease (CERAD; Mirra et al. 1991). Braak scores based on the staging of NFT pathology were established for each case (Braak and Braak 1991). Cases also received an NIA-Reagan Likelihood-of-AD diagnosis based on neuritic plaque and tangle pathology (Hyman and Trojanowski 1997). The "ABC" algorithm for the diagnosis of AD (Montine et al. 2012) is currently being applied to all RROS cases.

mRNA Extraction and Microarray Processing

Total RNA was isolated from frozen postmortem frontal cortex (BA 10) samples of NCI ($n = 13$), aMCI ($n = 11$), and mild/moderate AD ($n = 12$) cases that met inclusion/exclusion criteria. Tissue blocks (~50 mg) were excised on dry ice and, using best practices for RNA handling, total RNA was extracted from the tissue using the Ambion Total RNA Isolation Kit (Ambion/Life Technologies). Tissue was added to a 10× volume of the kit's lysis/binding buffer, and homogenates were prepared on ice using a Qiagen TissueLyser (Qiagen) set to 20 Hz for 1 min. Total RNA was extracted from the homogenate by phase separation using acid-phenol/chloroform. Sample quantification was performed by a Nanodrop spectrophotometer (ThermoFisher). RNA quality was assessed using an Agilent Bioanalyzer (Agilent) and all samples selected for analysis displayed RIN values ≥7. Double stranded cDNA was synthesized using a poly(A) primer to enrich for mRNA templating and subsequently labeled with Cy3 using Nimblegen's One-color DNA Labeling Kit (Roche Diagnostics); 4 ug of labeled cDNA was then hybridized to Nimblegen 12 × 135 K human arrays for 18 h at 42 °C. Analysis was performed on a GenePix 4200A scanner (Molecular Devices). Probe intensity levels were quantified with RMA preprocessing using NimbleScan v2.5 software. The microarray dataset has been uploaded to the Gene Expression Omnibus database (accession #GSE185909).

Weighted Gene Co-expression Network Analysis

Array-specific batch effects and variance attributable to postmortem interval (PMI) were removed via ComBat (Bioconductor, sva v3.4). WGCNA (v1.51) was used to group genes expressed similarly into modules following the workflow of Horvath and colleagues: (https://horvath.genetics.ucla.edu/html/CoexpressionNetwork/Rpackages/WGCNA/Tutorials/) (Langfelder and Horvath 2008). Briefly, power = 10 was chosen for the soft-thresholding as it achieved an R^2 of 0.8 and had high connectivity (mean $K = 136.0$). Color-coded modules whose eigen-genes had correlations >0.85 were combined to limit the total number of clusters examined. Spearman correlation was used to identify which modules and genes had evidence of being associated with the various diagnostic scales (nominal $P < 0.05$). Genes unassigned to any specific trait were grouped into the gray module. Heatmaps were used to visualize differences (Fig. 1). Geneset enrichment (MetaCore, Clarivate) was used to determine if modules were enriched for features relevant to clinical and/or pathological AD diagnostic criteria. Pathway hub genes were identified by MetaCore as genes with at least five edges in the pathway network. WGCNA hub genes were identified based on the highest kME, a measure of module connectivity (Langfelder and Horvath 2008). Finally, protein–protein interaction networks were created for each significant module by uploading their respective gene lists (gene symbols) to the STRING V11 database (Szklarczyk et al. 2019). The STRING database also provides gene ontology and KEGG pathway enrichment analyses, which were applied to each module and reported here in Tables 3 and 4, as well as Supplementary Table 1. Database sources that did not return significant results were not reported in the Tables. All statistical analyses were conducted using R v 3.3.2 (https://cran.r-project.org/).

Results

Subject Characteristics

Demographic, clinical, and neuropathological characteristics of the 36 RROS subjects are summarized in Table 1. There were no significant differences in age, sex, years of education, PMI, RIN values, or possession of at least one apolipoprotein (ApoE) $\varepsilon 4$ allele. In contrast, comparisons of clinical neuropathologic variables validated subject stratification into the three diagnostic groups. Subjects with AD had significantly lower MMSE scores ($P < 0.001$) and GCS ($P < 0.0001$) compared with the NCI and aMCI groups. Neuropathologically, the NCI group was quite heterogeneous and overlapped with the aMCI group, suggesting the presence of resilient subjects (Bennett et al. 2006; Mufson, Malek-Ahmadi, et al. 2016; Montine et al. 2019). For instance, NCI subjects met the criteria for Braak NFT stages I/II (31%) or III/IV (69%), whereas aMCI was categorized as Braak NFT stages I/II (36%) and III/IV (45%), or IV/V (19%). Distribution of Braak scores was significantly different between the AD and the NCI/aMCI groups ($P = 0.007$). In contrast, the AD group displayed a significantly greater degree of AD pathology than the NCI group based on NIA-Reagan criteria ($P = 0.007$), and CERAD neuritic plaque scores were higher in the AD group compared with the aMCI group ($P = 0.04$) (Table 1).

WGCNA and STRING Analysis of Microarray Data

WGCNA identified 3 modules out of 24 that were significantly correlated with clinical or neuropathological disease stage (Fig. 1). Significantly enriched pathways and hub genes for each of these modules are summarized in Table 2. The green module negatively correlated with clinical diagnostic group ($r = -0.33$, $P = 0.047$) and was significantly enriched for genes associated with insulin signaling. The midnight blue module positively correlated with both CERAD ($r = 0.34$, $P = 0.045$) and NIA-Reagan ($r = 0.38$, $P = 0.021$) diagnostic criteria and was enriched for genes associated with "cell adhesion related to platelet-endothelium-leucocyte interactions." Finally, the gray module, which represents genes that were unassigned to other modules and therefore not co-expressed, was nonetheless also positively associated with CERAD ($r = 0.43$, $P = 0.0084$) and NIA-Reagan ($r = 0.5$, $P = 0.021$) criteria, as well as with Braak NFT stage ($r = 0.51$, $P = 0.0015$). Genes in this module were significantly enriched for hypoxia and oxidative stress. None of the modules correlated with continuous variables including age, MMSE, or GCS (Fig. 1).

STRING network analysis was performed to predict physical interactions of the proteins encoded by each of the genes within each module that were significantly associated with any of the diagnostic scales (Szklarczyk et al. 2021). Of the 235 genes in the green module, STRING analysis identified 207 gene products/proteins with 131 interactions (Fig. 2), which was significantly more than the expected 90 ($P < 0.0001$). The insulin gene (*INS*) was the most integral part of the network with 14 different interactions, while cyclin-dependent kinase inhibitor 2 A (*CDKN2A*) had the second most interactions with eight (including *INS*); both are consistent with the hub genes identified via MetaCore. The STRING network analysis also determined that the green module was significantly enriched for five biological processes, four molecular functions, and the homeodomain (Table 3). Most of these enrichments were related to the regulation of transcription, which was intriguing given the identification of the zinc finger protein gene *ZNF837* as the top module hub gene via WGCNA (Table 2). Of the 80 genes in the midnight blue module, 68 encoded proteins and 23 interactions were identified via STRING. Despite no individual protein having more than two interactions, the midnight blue module had more interactions than what was expected in a set of proteins of similar size (14 expected edges, $P = 0.02$, Fig. 3). This module also had a greater number of significant enrichments than the green and gray modules, with the most notable being involved in G protein-coupled signaling and protein–protein binding

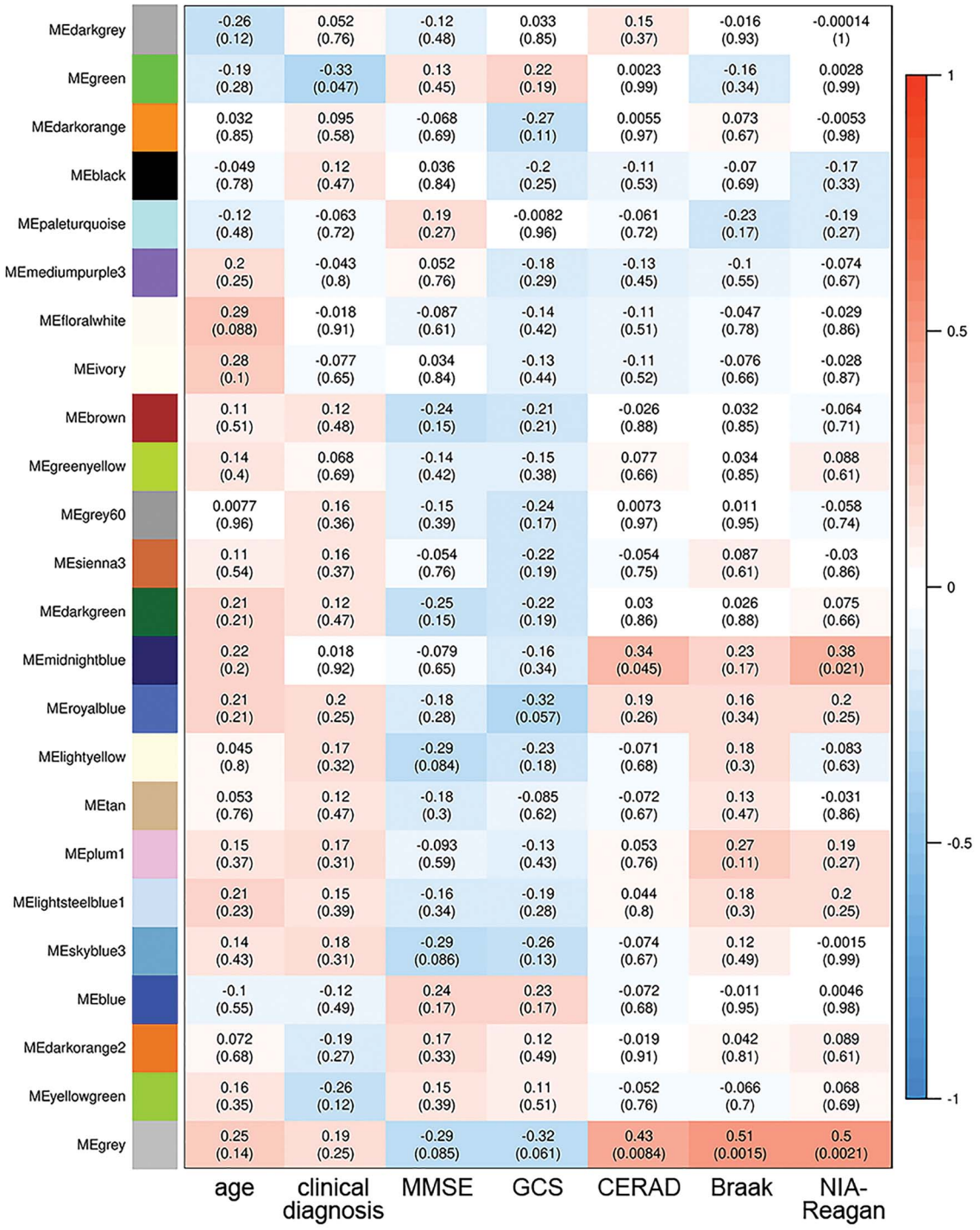

Figure 1. Identification of module-trait relationships of co-expressed genes in frontal cortex (BA 10) across the AD spectrum. Heatmap colored by the strength of the spearman correlation between each module's eigengene and demographic, clinical, or neuropathological variables. Shown are Spearman coefficients with *P*-values in parentheses.

(e.g., Kelch repeats) (Table 4). Olfaction and sensory perception were also enriched, consistent with the identification of the olfactory receptor gene *OR5D13* as the top module hub gene (Table 2). Finally, of the 28 genes in the gray module, which lacked co-expression, 26 encoded proteins and 2 interactions were identified, which was exactly the number of expected edges in a random set of 26 proteins (Supplementary Fig. 1). The gray module was significantly enriched for one molecular process and four protein domains related to glutathione S-transferase activity (Supplementary Table 1), which aligns with the module MetaCore pathway enrichment related to hypoxia and oxidative stress (Table 2). Finally, pair-wise comparisons of gene expression patterns among the three diagnostic groups are available in Supplementary Tables 2–4.

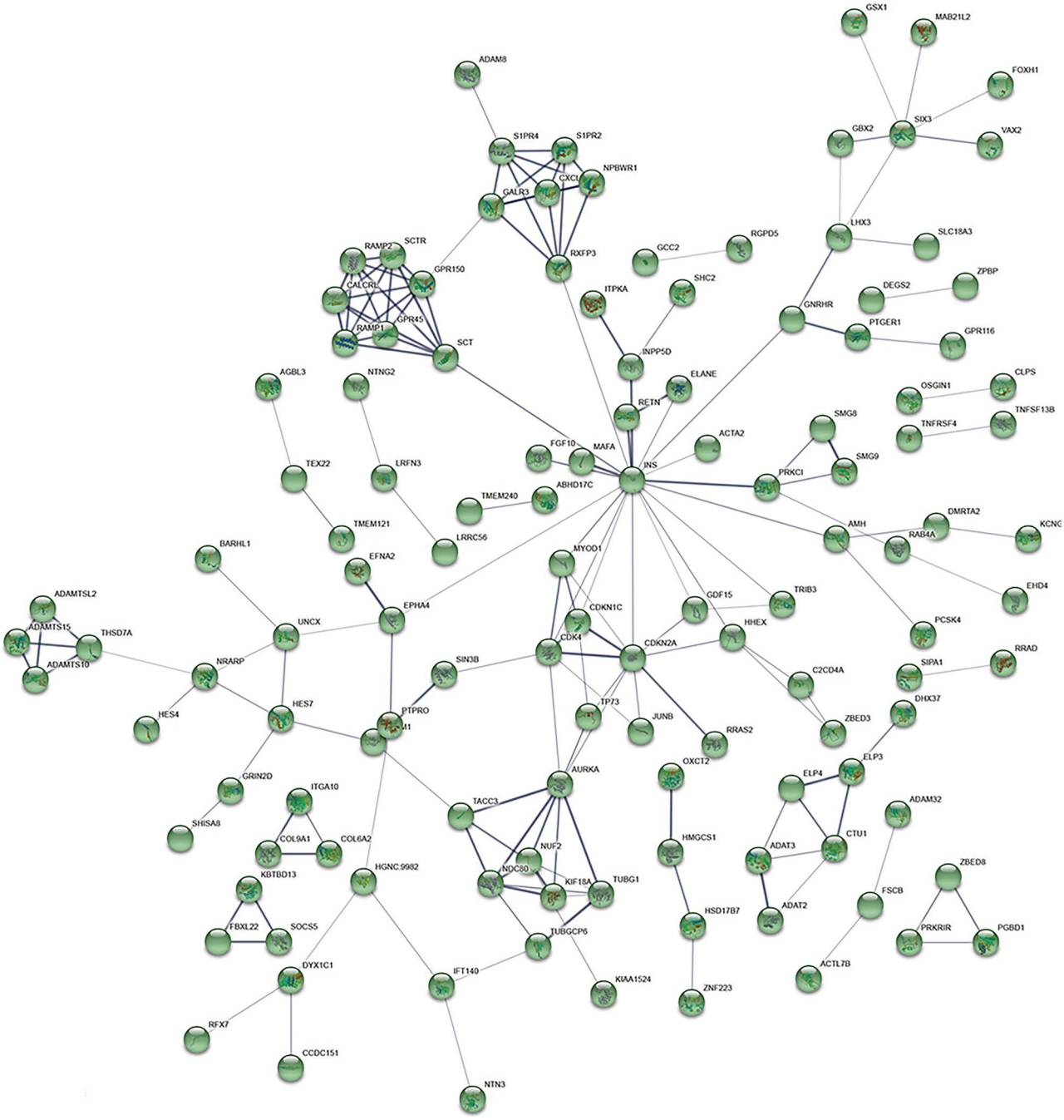

Figure 2. Protein–protein interactions in the green module associated with clinical diagnosis by STRING analysis. All 235 genes in the module were queried and only those with connectivity to at least one other gene are shown. *INS* and *CDKN2A* were the most connected genes in the module.

Discussion

The present study applied unbiased biological network analytical tools to a microarray dataset comparing gene expression profiles in frontal cortex from participants in the RROS who died with a range of cognitive abilities and neuropathological burden. The most compelling WGCNA outcome was the identification of 225 co-expressed genes within the green module that inversely correlated with clinical disease severity, as categorized by clinical diagnostic group (Fig. 1). MetaCore functional analysis revealed that insulin signaling was the only enriched pathway in this module (Table 2), whereas STRING network analysis showed that *INS* was the most highly connected gene in the module (Fig. 2, Table 3). Local brain insulin expression has been noted in rodent and human cerebral cortex and hippocampus (Grunblatt et al. 2007; Mehran et al. 2012; Csajbok et al. 2019), where it appears to be secreted by GABAergic neurogliaform cells (Molnar et al. 2014). Furthermore, type 2 diabetes mellitus (T2DM) is a risk factor for dementia, and AD progression is characterized by insulin resistance including defective brain insulin and insulin-like growth factor (IGF-1) signaling, as evidenced by reduced insulin receptor

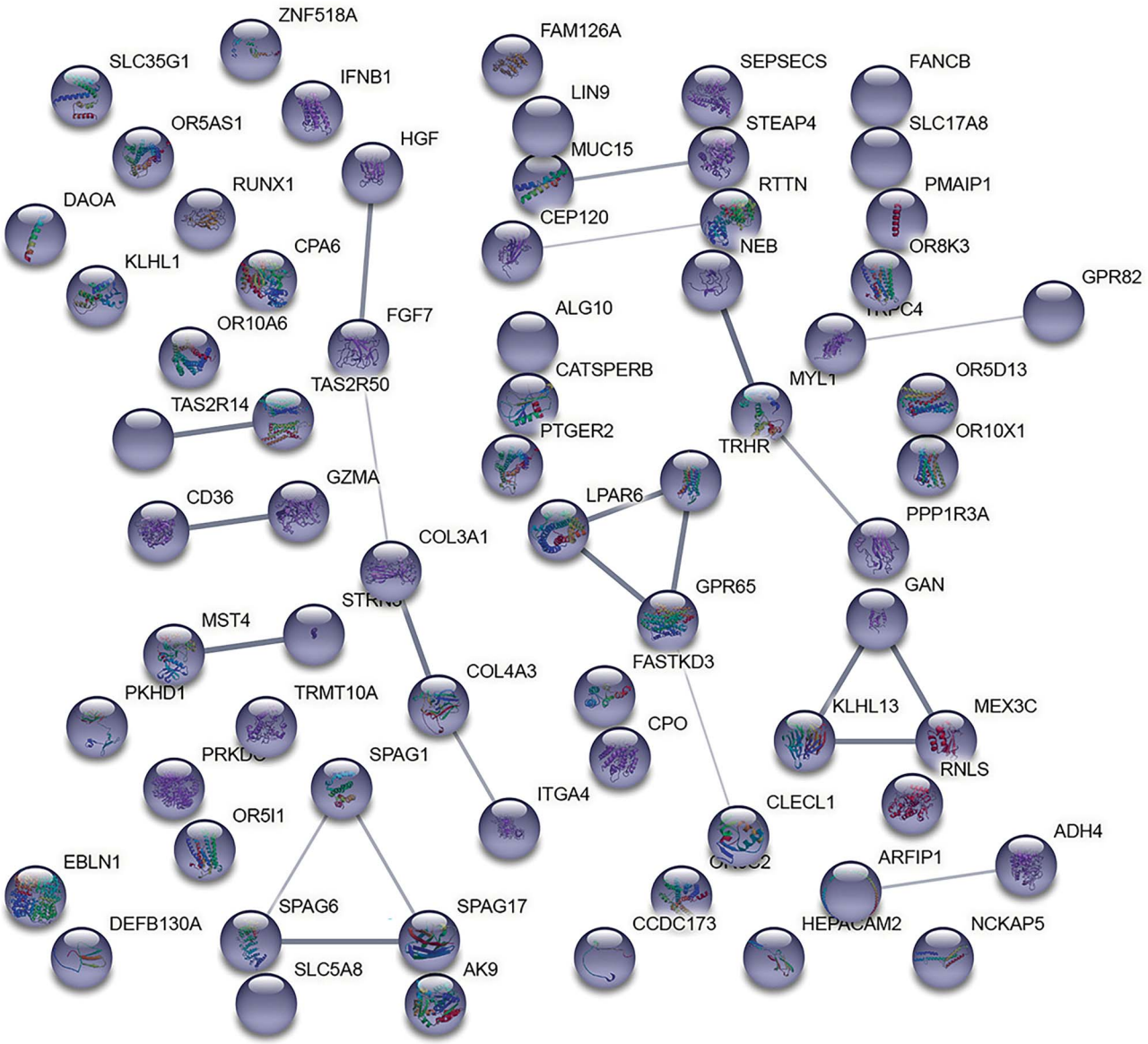

Figure 3. Protein–protein interactions in the midnight blue module associated with CERAD and NIA-Reagan diagnostic indices. All 80 genes in the module were queried.

binding and subsequent loss of insulin receptor substrate 1 and 2 activation and downstream Pi3K/Akt signaling (Talbot et al. 2012; Kellar and Craft 2020; Ferreira 2021). Moreover, insulin-sensitizing drugs have shown therapeutic promise for the disease (Arnold et al. 2018; Hayden et al. 2019). These data support the hypothesis that perturbations in insulin metabolism/signaling and brain insulin resistance are associated with the extent of cognitive impairment across the AD spectrum and may have diagnostic and therapeutic relevance in terms of generalized public health in the elderly. These changes in gene expression related to glucose utilization and energy metabolism could contribute to reductions in fluorodeoxyglucose positron emission tomography observed in the MCI and AD brain. Given recent evidence that microglial activation state may determine cerebral fluorodeoxyglucose uptake dynamics, it is also tempting to speculate that alterations in innate immunity may mediate the putative impact of *INS* signaling in the early stages of AD (Xiang et al. 2021).

Interestingly, the second most highly connected gene within the insulin pathway, *CDKN2A*, also plays an important role in the control of glucose and energy homeostasis in addition to its canonical role in cell cycle regulation (see below) (Drexler 1998). Loss-of-function mutations in this gene leading to haploinsufficiency affect glucose levels and insulin sensitivity (Pal et al. 2016; Kahoul et al. 2020), whereas genome wide association studies identified several single nucleotide polymorphisms (SNPs) in *CDKN2A* and upstream noncoding sequences that are risk factors for obesity and T2DM (Grant et al. 2010; Mehramiz et al. 2018; Kahoul et al. 2020). Specific SNPs in *CDKN2A* were associated with linkage of sporadic AD to chromosome 9 (Zuchner et al. 2008), although this association was not confirmed in a separate cohort (Tedde et al. 2011).

Table 1. Demographic, clinical, and neuropathological characteristics by diagnosis category

		Clinical diagnosis				
		NCI ($N = 13$)	aMCI ($N = 11$)	AD ($N = 12$)	P-value*	Pair-wise comparison
Age (years) at death:	Mean ± SD (Range)	83.9 ± 4.6 (76–92)	84.5 ± 5.5 (72–91)	87.0 ± 4.3 (80–94)	0.25[a]	—
Number (%) of males:		6 (46%)	5 (45%)	6 (50%)	0.64[b]	—
Years of education:	Mean ± SD (Range)	18.9 ± 2.9 (15–25)	19.3 ± 4.3 (8–23)	17.0 ± 2.0 (14–21)	0.21[a]	—
Number (%) with ApoE $\varepsilon 4$ allele:		2 (23%)	3 (27%)	3 (25%)	0.34[b]	—
MMSE:	Mean ± SD (Range)	28.3 ± 0.9 (27–30)	26.5 ± 1.4 (24–28)	17.4 ± 5.1 (10–27)	<0.0001[c]	(NCI, aMCI) > AD
GCS:	Mean ± SD (Range)	−0.02 ± 0.2 (−0.5–0.4)	−0.3 ± 0.3 (0.2–0.9)	−1.8 ± 0.6 (−2.5 to −0.8)	<0.0001[a]	(NCI, aMCI) > AD
PMI (h):	Mean ± SD (Range)	4.6 ± 3.0 (2.2–11.5)	5.8 ± 3.4 (2.7–13.0)	5.6 ± 3.3 (2.7–11.4)	0.73[c]	—
CERAD diagnosis:	No AD	3	4	1	0.04[c]	AD > aMCI
	Possible	5	3	2		
	Probable	5	2	5		
	Definite	0	2	4		
Distribution of Braak scores:	0	0	0	0	0.007[c]	AD > (NCI, aMCI)
	I/II	4	4	1		
	III/IV	9	5	4		
	V/VI	0	2	7		
NIA Reagan diagnosis (likelihood of AD):	No AD	1	0	0	0.007[c]	AD > NCI
	Low	6	4	1		
	Intermediate	6	6	7		
	High	0	1	4		
RIN values	Mean ± SD (Range)	7.4 ± 0.5 (7.0–8.3)	7.6 ± 0.4 (7.1–8.2)	7.5 ± 0.5 (7.0–8.4)	0.96[a]	—

[a]One-way ANOVA with Bonferroni correction for multiple comparisons. [b]Fisher's exact test with Bonferroni correction for multiple comparisons. [c]Kruskal–Wallis test with Dunn's test for multiple comparisons. [d]Parametric versus nonparametric analysis determined by Shapiro–Wilk test for normality.

Table 2. WGCNA summary

WGCNA module	Diagnostic category	MetaCore pathway enrichment	Pathway hub genes	WGCNA module top hub gene(s)
Green	Clinical diagnosis	Insulin signaling ($P = 0.016$)	*CDKN2A*, *CDKN2B*, *MYOD1*, *NAGLU*, *TP73*, *TEX22*	*ZNF837*
Midnight blue	CERAD, NIA-Reagan	Cell adhesion: platelet-endothelium-leucocyte interactions ($P = 0.05$)	*HGF*, *IFNB*, *ITGA4*, *PRKDC*, *PTGER2*, *RUNX1*	*OR5D13*
Gray	CERAD, Braak, NIA-Reagan	Response to hypoxia and oxidative stress ($P = 0.04$)	*ADAM10*, *CSMD3*, *ERBB4*, *ITGA6*	*AGPS*, *CNTN5**

Abbreviations: *ADAM10*, ADAM metallopeptidase domain 10; *AGPS*, alkylglycerone phosphate synthase; *CDKN2A*, cyclin dependent kinase inhibitor 2A; *CDKN2B*, cyclin dependent kinase inhibitor 2B; *CNTN5*, contactin 5; *CSMD3*, CUB and Sushi multiple domains 3; *ERBB4*, Erb-B2 receptor tyrosine kinase 4; *HGF*, hepatocyte growth factor; *IFNB*, interferon $\beta 1$, *ITGA4*, integrin subunit $\alpha 4$, *ITGA6*, integrin subunit $\alpha 6$; *MYOD1*, myogenic differentiation 1; *NAGLU*, N-acetyl-α-glucosaminidase; *OR5D13*, olfactory receptor family 5 subfamily D member 13; *TP73*, tumor protein 73; *PRKDC*, protein kinase, DNA-activated, catalytic subunit; *PTGER2*, prostaglandin E receptor 2; *RUNX1*, RUNX Family Transcription Factor 1; *TEX22*, testis expressed 22; *ZNF837*, zinc finger protein 837. [a]Tie for top hub gene in the module.

Table 3. Green module interactions—functional annotation

Enrichment type (database)	Description	Observed genes/background genes	Strength	P-value*
biological process (GO)	Pattern specification process	19/409	0.64	0.00041
	regionalization	14/313	0.63	0.0146
	regulation of transcription by RNA polymerase II	51/2633	0.26	0.0146
	regulation of transcription, DNA-templated	63/3661	0.21	0.0278
	anatomical structure morphogenesis	40/1992	0.28	0.0278
	tube development	22/793	0.42	0.0278
molecular function (GO)	transcription regulator activity	44/2069	0.3	0.003
	DNA-binding transcription factor activity, RNA polymerase II-specific	36/1633	0.32	0.0046
	DNA-binding transcription factor activity	38/1749	0.31	0.0046
	RNA polymerase II transcription regulatory region sequence-specific DNA binding	18/647	0.42	0.0276
protein domain (SMART)	homeodomain	10/241	0.59	0.0349

Abbreviations: GO, Gene Ontology; SMART, Simple Modular Architecture Research Tool. [a]Corrected via Benjamini–Hochberg False Discovery Rate (FDR).

Table 4. Midnight blue module interactions—functional annotation

Enrichment type (database)	Description	Observed genes/background genes	Strength	P-value*
Biological process (GO)	Sensory perception of chemical stimulus	10/487	0.77	0.0134
	detection of chemical stimulus involved in sensory perception	9/431	0.78	0.0175
	sensory perception	12/901	0.58	0.0223
	G protein-coupled receptor signaling pathway	14/1247	0.51	0.0256
	positive regulation of Rho protein signal transduction	3/28	1.49	0.0414
	mesenchymal-epithelial signaling	2/4	2.16	0.0414
Molecular function (GO)	G protein-coupled receptor activity	14/824	0.69	0.00024
	signaling receptor activity	17/1429	0.53	0.00084
	odorant binding	4/84	1.14	0.0136
	olfactory receptor activity	7/385	0.72	0.0187
Protein domain (InterPro)	G protein-coupled receptor, rhodopsin-like	12/668	0.71	0.00061
	GPCR, rhodopsin-like, 7TM	12/676	0.71	0.00061
	Olfactory receptor	7/384	0.72	0.0244
Protein domain (Pfam)	7 transmembrane receptor (rhodopsin family)	12/672	0.71	0.00033
	BTB and C-terminal Kelch	3/60	1.16	0.0266
	Galactose oxidase, central domain	3/44	1.29	0.0266
	Olfactory receptor	7/417	0.68	0.0266
	Kelch motif	3/52	1.22	0.0266
	Kelch motif	3/69	1.1	0.0306
	Zinc carboxypeptidase	2/23	1.4	0.0443
Protein domain (SMART)	Kelch	3/56	1.19	0.0427
	Zinc peptide	2/17	1.53	0.0427
	BTB and C-terminal Kelch	3/59	1.17	0.0427
Pathway (Reactome)	Signal Transduction	13/1358	0.44	0.0128
annotated keywords (UniPro)	G-protein-coupled receptor	14/778	0.71	0.0000766
	Glycoprotein	32/4352	0.33	0.00033
	Receptor	17/1423	0.54	0.00033
	Sensory transduction	9/560	0.67	0.0051
	Olfaction	7/396	0.71	0.014
	Cell membrane	22/3214	0.29	0.0238
	Kelch repeat	3/71	1.08	0.0473

Abbreviations: GO, Gene Ontology; Pfam, Protein family; SMART, Simple Modular Architecture Research Tool. [a]Corrected via Benjamini–Hochberg FDR.

With respect to cell cycle regulation, *CDKN2A*—along with pathway genes *CDKN2B* and *MYOD1*—are functionally implicated in maintaining cell cycle arrest at G1 and a differentiated cellular phenotype (Drexler 1998; Sabourin et al. 1999). Given the negative correlation between the green module and clinical severity, dysregulation of these genes could be related to markers of aneuploidy and aberrant cell cycle re-entry that have long been observed in selectively vulnerable neurons in postmortem AD brain tissue (Vincent et al. 1996; Herrup and Arendt 2002; Park et al. 2007). Intriguingly, insulin/IGF-1 signaling also has been linked to cell cycle regulation and oncogenesis in peripheral cells (Teng et al. 1976; Lai et al. 2001; Mairet-Coello et al.

2009). Pathway correlations with *NAGLU*, which degrades heparin sulfate (Yogalingam et al. 2000), are interesting given observations that T2DM is associated with reduced heparin sulfate levels (Rohrbach et al. 1982; Makino et al. 1992), thus impacting basement membrane permeability and coagulation (Shionoya 1927).

Mechanisms underlying the potential association of insulin signaling pathways with clinical disease progression are not clear, yet STRING interactome analysis highlighted transcriptional regulation as a major node of the enriched molecular and biological processes connecting module genes, and the homeodomain was the only protein domain identified (Table 3). This theme was complemented by processes related to pattern specification, suggesting that disturbances in coordinated genomic and transcriptional regulatory sequences in frontal cortex may contribute to putative insulin signaling and related pathway (e.g., cell cycle regulation or heparin metabolism) dysfunction during AD progression. Interestingly, the most highly correlated green module hub gene was *ZNF837*, a member of the C2H2-type-zinc finger family of transcription factors (Fedotova et al. 2017). While the protein function of this specific *ZNF* gene is unknown, the presence of the zinc finger motif is associated with diverse functions including transcription, mRNA trafficking, zinc and iron-sensing, ubiquitin-mediated protein degradation, cytoskeletal function, DNA repair, and cell adhesion (Laity et al. 2001).

In contrast to the green module, two additional modules were positively associated with increasing amyloid and tau pathology. The midnight blue module correlated with CERAD and NIA-Reagan diagnostic criteria ($P < 0.05$), and "cell adhesion related to platelet-endothelium-leucocyte interactions" emerged as the only significantly enriched pathway via MetaCore (Table 2). The prominence of this functional network in the module may provide additional insights for the growing literature implicating vascular integrity in disease progression (Hachinski et al. 2019; Carare et al. 2020). Leucocyte adhesion to the vascular endothelium is a hallmark of the inflammatory process (Wahl et al. 1996), leveraging the sequential activation and binding of adhesion molecules and their receptors for transendothelial migration into the interstitium. In contrast, platelet adhesion to activated endothelial cells is a hallmark of hemostasis following vascular injury (Margraf and Zarbock 2019). Among the pathway hub genes identified, *ITGA4* is a ubiquitous integrin subunit expressed by immune cells and has been implicated in mediating leukocyte-endothelium adhesion (Luissint et al. 2008), while *HGF* and *INFB* are multifunctional cytokines implicated in innate immune responses and tissue repair (Le Page et al. 2000; Mungunsukh et al. 2014). Significantly, the prostaglandin E2 (PE2) receptor encoded by *PTGER2* is implicated in AD since microglial PE2—a metabolite of arachidonic acid—has been identified as a participant in context-dependent pro- and anti-inflammatory signaling pathways during the early stages of AD progression (Johansson et al. 2015; Pradhan et al. 2017).

STRING interactome analysis revealed relatively poor connectivity within this module (Fig. 3), suggesting a disruption of parallel rather than interconnected pathways associated with putative adhesion dysfunction. However, G protein-coupled receptor activity and signal transduction were major themes of the enriched molecular and biological processes, whereas enriched protein domains included protein–protein binding motifs such as Kelch motifs, which have been shown to regulate receptor activity (Marshall et al. 2011) (Table 4). Curiously, sensory perception processes were also identified, and the most highly correlated gene in the midnight blue module was *OR5D13*, a segregating gene/pseudogene (i.e., expressing functional, protein-encoding, and nonfunctional alleles) member of the G protein-coupled olfactory receptor superfamily. The association of a chemosensory gene with expression profiles in frontal cortex seems counterintuitive, but a recent longitudinal study of archived diffusion-weighted imaging and GWAS datasets from ADNI identified SNPs in *OR5D13*, as well as several other *OR* genes, as among the top 30 genetic variants associated with changes in global structural connectivity across subjects with NCI, MCI, or AD (Elsheikh et al. 2020). The expression of olfactory receptors in multiple peripheral and central tissues suggests that this diverse family of receptors responds to different ligands in a context-dependent manner beyond their role in odorant detection (Ferrer et al. 2016). For instance, in vitro and in vivo studies have shown that olfactory receptors regulate 1) the induction of cell adhesion in both homo- and heterotypic receptor expression paradigms (Richard et al. 2013) and 2) myocyte migration and adhesion during myogenesis and fiber branching (Griffin et al. 2009).

Gene expression in the gray module was positively associated with CERAD, NIA-Reagan, and Braak NFT diagnostic criteria ($P < 0.04$), with pathway enrichment for responses to hypoxia and oxidative stress. This is particularly intriguing since this module represents genes that were unassigned to the other modules. This finding may indicate an overrepresentation of genes correlating positively with increasing pathological severity that are involved in regulating pathways such as respiration and redox homeostasis. The identification of biological and molecular processes related to glutathione S-transferase activity by STRING analysis (Supplementary Table 1) supports this possibility (Jakoby 1978). The extent of cerebrovascular lesions has been increasingly recognized as a driving force in mediating the impact of global pathological change on the onset and extent of cognitive impairment (Arvanitakis et al. 2011), whereas oxidative stress—whether as a result of local hypoxic events or metabolic dysregulation—has long been recognized as an

important effector pathway during disease progression (Lovell and Markesbery 2007).

To our knowledge, this is the first WGCNA of brain tissue expression profiles using the well-established RROS cohort to identify these three specific pathways associated with clinical neuropathologic disease severity during the progression of AD. Moreover, they may represent key processes impacting the integrity of frontal cortex activity in mediating executive function and the performance of higher cognitive connectomes such as the default mode network. Notably, a recent WGCNA of microarray data from control, MCI, and AD whole blood samples revealed that modules correlated to diagnostic progression with pathway enrichment for increased insulin resistance, leukocyte transendothelial migration, and "positive regulation of oxidative stress-induced neuron death (Tang and Liu 2019)." This supports our findings and suggests that the detection of novel molecules in peripheral fluid that are involved in these pathways may be candidate biomarkers of disease.

Our results are also consistent with other WGCNA studies related to AD that found only a single or few number of total modules significantly associated with clinical diagnostic group (Tao et al. 2020; Qin et al. 2021; Wang et al. 2021; Zhou et al. 2021; Zhang, Liu, et al. 2021) or neuropathologic diagnostic criteria (Sun et al. 2019; Zhang, Shen, et al. 2021). In contrast, two additional studies have also identified modules associated with MMSE scores (Liang et al. 2018; Sun et al. 2019). The main pathways associated with these modules include proteasome structure and function (e.g., *PSMA4*), signal transduction (e.g., *GRIK1*) and trafficking (e.g., *RAB31*), chaperones (e.g., *DNAJA1*), ribosome structure and function (e.g., *RPS3A*), oxidative stress (e.g., metallothioniens *MT1* and *MT2*), and CNS development (e.g., *NOTCH2*) (Liang et al. 2018; Sun et al. 2019; Milind et al. 2020; Tao et al. 2020; Zhang, Liu, et al. 2021), thus highlighting the relative novelty of the present report. The reasons why our study did not identify these pathways and/or hub genes, or why our significantly correlated modules were not associated with MMSE or the RROS-specific GSC, are unclear. However, these differences may relate to: 1) our focus on BA10, which is unique to date; 2) our relatively stringent inclusion/exclusion criteria; or 3) differences in significant results based upon false-rate discovery algorithms applied to variable numbers of groups, sample sizes, and different microarray platforms across these studies.

A caveat for the present study is that a significant proportion of NCI subjects displayed high AD pathology, so we cannot rule out the possibility that many of the co-expressed gene families correlating with clinical or pathological disease progression reflected compensatory responses related to resilience, in addition to those associated with disease pathogenesis. Future directions will: 1) perform studies with increased power to differentiate gene expression patterns in high- and low-pathology NCI in relation to MCI and AD as a strategy for further pinpointing markers of resilience; and 2) seek to validate and understand the biological and mechanistic significance of these co-expressed gene networks in AD beyond their statistical correlation with diagnostic variables, which may also prove to have diagnostic and/or therapeutic implications.

Supplementary Material

Supplementary material can be found at *Cerebral Cortex* online.

Abbreviation List

Aβ, Amyloid-β; *ADAM10*, ADAM metallopeptidase domain 10; AD, Alzheimer's disease; ADNI, AD neuroimaging initiative; aMCI, Amnestic mild cognitive impairment; *AGPS*, Alkylglycerone phosphate synthase; apoE, Apolipoprotein E; *BACE1*, β-secretase 1; *CDKN2A*, Cyclin dependent kinase inhibitor 2A; *CDKN2B*, Cyclin dependent kinase inhibitor 2B; CERAD, Consortium to Establish a Registry for Alzheimer's Disease; *CNTN5*, Contactin 5; *CSMD3*, CUB and Sushi multiple domains 3; *DNAJA1*, DnaJ Heat Shock Protein Family (Hsp40) Member A; *ERBB4*, Erb-B2 receptor tyrosine kinase 4; GCS, Global cognitive score; *GRIK1*, Glutamate Ionotropic Receptor Kainate Type Subunit 1; GWAS, Genome-wise association study; *HGF*, Hepatocyte growth factor; *IFNB*, Interferon β1; IGF-1, Insulin-like growth factor; *INS*, Insulin; *ITGA4*, Integrin subunit α4; *ITGA6*, Integrin subunit α6; MMSE, Mini-mental state exam; *MYOD1*, Myogenic differentiation 1; *MT1/MT2*, Metallothionein 1/2; *NAGLU*, N-acetyl-α-glucosaminidase; NCI, No cognitive impairment; NFT, Neurofibrillary tangle; *NOTCH2*, Notch receptor 2; *ORD5D13*, Olfactory receptor family 5 subfamily D member 13; PMI, Postmortem interval; *PRKDC*, Protein kinase; DNA-activated; Catalytic subunit; *PSMA4*, Proteasome 20S Subunit Alpha 4; *PTGER2*, Prostaglandin E receptor 2; *RAB31*, RAB31 Member RAS Oncogene Family; *RUNX1*, RUNX Family Transcription Factor 1; RROS, Rush Religious Orders Study; *RPS3A*, Ribosomal Protein S3A; SNP, Single nucleotide polymorphism; *TEX22*, Testis expressed 22; T2DM, Type 2 diabetes mellitus; *TP73*, Tumor protein 73; *ZNF837*, Zinc finger protein 837

Funding

National Institute on Aging at the National Institute of Health (grants P01 AG014449, P30 AG010161, P30 AG053760, P01 AG017617, R56 AG072599, R01 AG060731, R01 AG043375, R01 AG062217); Spectrum Health-MSU Alliance Corporation.

Notes

The authors are grateful for the altruism of RROS participants. *Conflict of Interest*: None declared.

References

Abner EL, Kryscio RJ, Cooper GE, Fardo DW, Jicha GA, Mendiondo MS, Nelson PT, Smith CD, Van Eldik LJ, Wan L, et al. 2012. Mild cognitive impairment: statistical models of transition using longitudinal clinical data. *Int J Alzheimers Dis*. 2012:291920.

Alldred MJ, Penikalapati SC, Lee SH, Heguy A, Roussos P, Ginsberg SD. 2021. Profiling basal forebrain cholinergic neurons reveals a molecular basis for vulnerability within the Ts65Dn model of down syndrome and Alzheimer's disease. *Mol Neurobiol*. 58: 5141–5162.

Arnold SE, Arvanitakis Z, Macauley-Rambach SL, Koenig AM, Wang HY, Ahima RS, Craft S, Gandy S, Buettner C, Stoeckel LE, et al. 2018. Brain insulin resistance in type 2 diabetes and Alzheimer disease: concepts and conundrums. *Nat Rev Neurol*. 14:168–181.

Arvanitakis Z, Leurgans SE, Barnes LL, Bennett DA, Schneider JA. 2011. Microinfarct pathology, dementia, and cognitive systems. *Stroke*. 42:722–727.

Bell KF, Bennett DA, Cuello AC. 2007. Paradoxical upregulation of glutamatergic presynaptic boutons during mild cognitive impairment. *J Neurosci*. 27:10810–10817.

Bennett DA, Wilson RS, Schneider JA, Evans DA, Beckett LA, Aggarwal NT, Barnes LL, Fox JH, Bach J. 2002. Natural history of mild cognitive impairment in older persons. *Neurology*. 59:198–205.

Bennett DA, Schneider JA, Arvanitakis Z, Kelly JF, Aggarwal NT, Shah RC, Wilson RS. 2006. Neuropathology of older persons without cognitive impairment from two community-based studies. *Neurology*. 66:1837–1844.

Bossers K, Wirz KT, Meerhoff GF, Essing AH, van Dongen JW, Houba P, Kruse CG, Verhaagen J, Swaab DF. 2010. Concerted changes in transcripts in the prefrontal cortex precede neuropathology in Alzheimer's disease. *Brain*. 133:3699–3723.

Braak H, Braak E. 1991. Neuropathological stageing of Alzheimer-related changes. *Acta Neuropathol*. 82:239–259.

Carare RO, Aldea R, Agarwal N, Bacskai BJ, Bechman I, Boche D, Bu G, Bulters D, Clemens A, Counts SE, et al. 2020. Clearance of interstitial fluid (ISF) and CSF (CLIC) group-part of vascular professional interest area (PIA): cerebrovascular disease and the failure of elimination of amyloid-beta from the brain and retina with age and Alzheimer's disease-opportunities for therapy. *Alzheimers Dement*. 12:e12053.

Counts SE, Nadeem M, Lad SP, Wuu J, Mufson EJ. 2006. Differential expression of synaptic proteins in the frontal and temporal cortex of elderly subjects with mild cognitive impairment. *J Neuropathol Exp Neurol*. 65:592–601.

Counts SE, Alldred MJ, Che S, Ginsberg SD, Mufson EJ. 2013. Synaptic gene dysregulation within hippocampal CA1 pyramidal neurons in mild cognitive impairment. *Neuropharmacology*. 79C:172–179.

Csajbok EA, Kocsis AK, Farago N, Furdan S, Kovacs B, Lovas S, Molnar G, Liko I, Zvara A, Puskas LG, et al. 2019. Expression of GLP-1 receptors in insulin-containing interneurons of rat cerebral cortex. *Diabetologia*. 62:717–725.

DeKosky ST, Ikonomovic MD, Styren SD, Beckett L, Wisniewski S, Bennett DA, Cochran EJ, Kordower JH, Mufson EJ. 2002. Upregulation of choline acetyltransferase activity in hippocampus and frontal cortex of elderly subjects with mild cognitive impairment. *Ann Neurol*. 51:145–155.

DeSerisy M, Ramphal B, Pagliaccio D, Raffanello E, Tau G, Marsh R, Posner J, Margolis AE. 2021. Frontoparietal and default mode network connectivity varies with age and intelligence. *Dev Cogn Neurosci*. 48:100928.

Dillen KNH, Jacobs HIL, Kukolja J, Richter N, von Reutern B, Onur OA, Langen KJ, Fink GR. 2017. Functional disintegration of the default mode network in prodromal Alzheimer's disease. *J Alzheimers Dis*. 59:169–187.

Drexler HG. 1998. Review of alterations of the cyclin-dependent kinase inhibitor INK4 family genes p15, p16, p18 and p19 in human leukemia-lymphoma cells. *Leukemia*. 12:845–859.

Dunckley T, Beach TG, Ramsey KE, Grover A, Mastroeni D, Walker DG, LaFleur BJ, Coon KD, Brown KM, Caselli R, et al. 2006. Gene expression correlates of neurofibrillary tangles in Alzheimer's disease. *Neurobiol Aging*. 27:1359–1371.

Elsheikh SSM, Chimusa ER, Mulder NJ, Crimi A. 2020. Genome-wide association study of brain connectivity changes for Alzheimer's disease. *Sci Rep*. 10:1433.

Fedotova AA, Bonchuk AN, Mogila VA, Georgiev PG. 2017. C2H2 zinc finger proteins: the largest but poorly explored family of higher eukaryotic transcription factors. *Acta Nat*. 9:47–58.

Ferreira ST. 2021. Brain insulin, insulin-like growth factor 1 and glucagon-like peptide 1 signalling in Alzheimer's disease. *J Neuroendocrinol*. 33:e12959.

Ferrer I, Garcia-Esparcia P, Carmona M, Carro E, Aronica E, Kovacs GG, Grison A, Gustincich S. 2016. Olfactory receptors in non-chemosensory organs: the nervous system in health and disease. *Front Aging Neurosci*. 8:163.

Ginsberg SD, Che S, Wuu J, Counts SE, Mufson EJ. 2006. Down regulation of trk but not p75NTR gene expression in single cholinergic basal forebrain neurons mark the progression of Alzheimer's disease. *J Neurochem*. 97:475–487.

Grant SF, Hakonarson H, Schwartz S. 2010. Can the genetics of type 1 and type 2 diabetes shed light on the genetics of latent autoimmune diabetes in adults? *Endocr Rev*. 31:183–193.

Griffin CA, Kafadar KA, Pavlath GK. 2009. MOR23 promotes muscle regeneration and regulates cell adhesion and migration. *Dev Cell*. 17:649–661.

Grunblatt E, Salkovic-Petrisic M, Osmanovic J, Riederer P, Hoyer S. 2007. Brain insulin system dysfunction in streptozotocin intracerebroventricularly treated rats generates hyperphosphorylated tau protein. *J Neurochem*. 101:757–770.

Hachinski V, Einhaupl K, Ganten D, Alladi S, Brayne C, Stephan BCM, Sweeney MD, Zlokovic B, Iturria-Medina Y, Iadecola C, et al. 2019. Preventing dementia by preventing stroke: the berlin manifesto. *Alzheimers Dement*. 15:961–984.

Hayden MR, Grant DG, Aroor AR, DeMarco VG. 2019. Empagliflozin ameliorates type 2 diabetes-induced ultrastructural remodeling of the neurovascular unit and neuroglia in the female db/db mouse. *Brain Sci*. 9:57.

Herrup K, Arendt T. 2002. Re-expression of cell cycle proteins induces neuronal cell death during Alzheimer's disease. *J Alzheimers Dis*. 4:243–247.

Hyman BT, Trojanowski JQ. 1997. Consensus recommendations for the postmortem diagnosis of Alzheimer disease from the National Institute on Aging and the Reagan Institute Working Group on diagnostic criteria for the neuropathological assessment of Alzheimer disease. *J Neuropathol Exp Neurol*. 56:1095–1097.

Hyman BT, Phelps CH, Beach TG, Bigio EH, Cairns NJ, Carrillo MC, Dickson DW, Duyckaerts C, Frosch MP, Masliah E, et al. 2012. National Institute on Aging-Alzheimer's Association guidelines for the neuropathologic assessment of Alzheimer's disease. *Alzheimers Dement*. 8:1–13.

Jack CR Jr, Bennett DA, Blennow K, Carrillo MC, Feldman HH, Frisoni GB, Hampel H, Jagust WJ, Johnson KA, Knopman DS, et al. 2016. A/T/N: an unbiased descriptive classification scheme for Alzheimer disease biomarkers. *Neurology*. 87:539–547.

Jack CR Jr, Bennett DA, Blennow K, Carrillo MC, Dunn B, Haeberlein SB, Holtzman DM, Jagust W, Jessen F, Karlawish J, et al. 2018.

NIA-AA research framework: toward a biological definition of Alzheimer's disease. *Alzheimers Dement*. 14:535–562.

Jakoby WB. 1978. The glutathione S-transferases: a group of multifunctional detoxification proteins. *Adv Enzymol Relat Areas Mol Biol*. 46:383–414.

Johansson JU, Woodling NS, Shi J, Andreasson KI. 2015. Inflammatory cyclooxygenase activity and PGE2 Signaling in models of Alzheimer's disease. *Curr Immunol Rev*. 11:125–131.

Kahoul Y, Oger F, Montaigne J, Froguel P, Breton C, Annicotte JS. 2020. Emerging roles for the INK4a/ARF (CDKN2A) locus in adipose tissue: implications for obesity and type 2 diabetes. *Biomol Ther*. 10:1350.

Kellar D, Craft S. 2020. Brain insulin resistance in Alzheimer's disease and related disorders: mechanisms and therapeutic approaches. *Lancet Neurol*. 19:758–766.

Kelly SC, He B, Perez SE, Ginsberg SD, Mufson EJ, Counts SE. 2017. Locus coeruleus cellular and molecular pathology during the progression of Alzheimer's disease. *Acta Neuropathol Commun*. 5:8.

Lai A, Sarcevic B, Prall OW, Sutherland RL. 2001. Insulin/insulin-like growth factor-I and estrogen cooperate to stimulate cyclin E-Cdk2 activation and cell cycle progression in MCF-7 breast cancer cells through differential regulation of cyclin E and p21(WAF1/Cip1). *J Biol Chem*. 276:25823–25833.

Laity JH, Lee BM, Wright PE. 2001. Zinc finger proteins: new insights into structural and functional diversity. *Curr Opin Struct Biol*. 11: 39–46.

Langfelder P, Horvath S. 2008. WGCNA: an R package for weighted correlation network analysis. *BMC Bioinformatics*. 9:559.

Le Page C, Genin P, Baines MG, Hiscott J. 2000. Interferon activation and innate immunity. *Rev Immunogenet*. 2:374–386.

Liang JW, Fang ZY, Huang Y, Liuyang ZY, Zhang XL, Wang JL, Wei H, Wang JZ, Wang XC, Zeng J, et al. 2018. Application of weighted gene co-expression network analysis to explore the key genes in Alzheimer's disease. *J Alzheimers Dis*. 65:1353–1364.

Liu H, Qin W, Li W, Fan L, Wang J, Jiang T, Yu C. 2013. Connectivity-based parcellation of the human frontal pole with diffusion tensor imaging. *J Neurosci*. 33:6782–6790.

Lovell MA, Markesbery WR. 2007. Oxidative damage in mild cognitive impairment and early Alzheimer's disease. *J Neurosci Res*. 85: 3036–3040.

Luissint AC, Lutz PG, Calderwood DA, Couraud PO, Bourdoulous S. 2008. JAM-L-mediated leukocyte adhesion to endothelial cells is regulated in cis by alpha4beta1 integrin activation. *J Cell Biol*. 183: 1159–1173.

Mairet-Coello G, Tury A, DiCicco-Bloom E. 2009. Insulin-like growth factor-1 promotes G(1)/S cell cycle progression through bidirectional regulation of cyclins and cyclin-dependent kinase inhibitors via the phosphatidylinositol 3-kinase/Akt pathway in developing rat cerebral cortex. *J Neurosci*. 29:775–788.

Makino H, Ikeda S, Haramoto T, Ota Z. 1992. Heparan sulfate proteoglycans are lost in patients with diabetic nephropathy. *Nephron*. 61:415–421.

Margraf A, Zarbock A. 2019. Platelets in inflammation and resolution. *J Immunol*. 203:2357–2367.

Marshall J, Blair LA, Singer JD. 2011. BTB-Kelch proteins and ubiquitination of kainate receptors. *Adv Exp Med Biol*. 717:115–125.

McKhann GM, Knopman DS, Chertkow H, Hyman BT, Jack CR Jr, Kawas CH, Klunk WE, Koroshetz WJ, Manly JJ, Mayeux R, et al. 2011. The diagnosis of dementia due to Alzheimer's disease: recommendations from the National Institute on Aging-Alzheimer's Association workgroups on diagnostic guidelines for Alzheimer's disease. *Alzheimers Dement*. 7:263–269.

Mehramiz M, Ghasemi F, Esmaily H, Tayefi M, Hassanian SM, Sadeghzade M, Sadabadi F, Moohebati M, Azarpazhooh MR, Parizadeh SMR, et al. 2018. Interaction between a variant of CDKN2A/B-gene with lifestyle factors in determining dyslipidemia and estimated cardiovascular risk: a step toward personalized nutrition. *Clin Nutr*. 37:254–261.

Mehran AE, Templeman NM, Brigidi GS, Lim GE, Chu KY, Hu X, Botezelli JD, Asadi A, Hoffman BG, Kieffer TJ, et al. 2012. Hyperinsulinemia drives diet-induced obesity independently of brain insulin production. *Cell Metab*. 16:723–737.

Milind N, Preuss C, Haber A, Ananda G, Mukherjee S, John C, Shapley S, Logsdon BA, Crane PK, Carter GW. 2020. Transcriptomic stratification of late-onset Alzheimer's cases reveals novel genetic modifiers of disease pathology. *PLoS Genet*. 16: e1008775.

Miller JA, Woltjer RL, Goodenbour JM, Horvath S, Geschwind DH. 2013. Genes and pathways underlying regional and cell type changes in Alzheimer's disease. *Genome Med*. 5:48.

Mirra SS, Heyman A, McKeel D, Sumi SM, Crain BJ, Brownlee LM, Vogel FS, Hughes JP, van Belle G, Berg L. 1991. The consortium to establish a registry for Alzheimer's disease (CERAD). Part II. Standardization of the neuropathologic assessment of Alzheimer's disease. *Neurology*. 41:479–486.

Moayedi M, Salomons TV, Dunlop KA, Downar J, Davis KD. 2015. Connectivity-based parcellation of the human frontal polar cortex. *Brain Struct Funct*. 220:2603–2616.

Molnar G, Farago N, Kocsis AK, Rozsa M, Lovas S, Boldog E, Baldi R, Csajbok E, Gardi J, Puskas LG, et al. 2014. GABAergic neurogliaform cells represent local sources of insulin in the cerebral cortex. *J Neurosci*. 34:1133–1137.

Montine TJ, Phelps CH, Beach TG, Bigio EH, Cairns NJ, Dickson DW, Duyckaerts C, Frosch MP, Masliah E, Mirra SS, et al. 2012. National Institute on Aging-Alzheimer's Association guidelines for the neuropathologic assessment of Alzheimer's disease: a practical approach. *Acta Neuropathol*. 123:1–11.

Montine TJ, Cholerton BA, Corrada MM, Edland SD, Flanagan ME, Hemmy LS, Kawas CH, White LR. 2019. Concepts for brain aging: resistance, resilience, reserve, and compensation. *Alzheimers Res Ther*. 11:22.

Morris JC, Storandt M, Miller JP, McKeel DW, Price JL, Rubin EH, Berg L. 2001. Mild cognitive impairment represents early-stage Alzheimer disease. *Arch Neurol*. 58:397–405.

Mufson EJ, Ikonomovic MD, Counts SE, Perez SE, Malek-Ahmadi M, Scheff SW, Ginsberg SD. 2016. Molecular and cellular pathophysiology of preclinical Alzheimer's disease. *Behav Brain Res*. 311: 54–69.

Mufson EJ, Malek-Ahmadi M, Perez SE, Chen K. 2016. Braak staging, plaque pathology, and APOE status in elderly persons without cognitive impairment. *Neurobiol Aging*. 37:147–153.

Mungunsukh O, McCart EA, Day RM. 2014. Hepatocyte growth factor isoforms in tissue repair, cancer, and fibrotic remodeling. *Biomedicine*. 2:301–326.

Pal A, Potjer TP, Thomsen SK, Ng HJ, Barrett A, Scharfmann R, James TJ, Bishop DT, Karpe F, Godsland IF, et al. 2016. Loss-of-function mutations in the cell-cycle control gene CDKN2A impact on glucose homeostasis in humans. *Diabetes*. 65:527–533.

Park KH, Hallows JL, Chakrabarty P, Davies P, Vincent I. 2007. Conditional neuronal simian virus 40 T antigen expression induces Alzheimer-like tau and amyloid pathology in mice. *J Neurosci*. 27: 2969–2978.

Petersen RC. 2004. Mild cognitive impairment as a diagnostic entity. *J Intern Med*. 256:183–194.

Pradhan SS, Salinas K, Garduno AC, Johansson JU, Wang Q, Manning-Bog A, Andreasson KI. 2017. Anti-inflammatory and neuroprotective effects of PGE2 EP4 signaling in models of Parkinson's disease. *J NeuroImmune Pharmacol*. 12:292–304.

Qin H, Hu C, Zhao X, Tian M, Zhu B. 2021. Usefulness of candidate mRNAs and miRNAs as biomarkers for mild cognitive impairment and Alzheimer's disease. *Int J Neurosci*. 1–14. https://doi.org/10.1080/00207454.2021.1886098. Online ahead of print.

Richard M, Jamet S, Fouquet C, Dubacq C, Boggetto N, Pincet F, Gourier C, Trembleau A. 2013. Homotypic and heterotypic adhesion induced by odorant receptors and the beta2-adrenergic receptor. *PLoS One*. 8:e80100.

Rohrbach DH, Hassell JR, Kleinman HK, Martin GR. 1982. Alterations in the basement membrane (heparan sulfate) proteoglycan in diabetic mice. *Diabetes*. 31:185–188.

Sabourin LA, Girgis-Gabardo A, Seale P, Asakura A, Rudnicki MA. 1999. Reduced differentiation potential of primary MyoD−/− myogenic cells derived from adult skeletal muscle. *J Cell Biol*. 144: 631–643.

Schneider JA, Arvanitakis Z, Leurgans SE, Bennett DA. 2009. The neuropathology of probable Alzheimer disease and mild cognitive impairment. *Ann Neurol*. 66:200–208.

Seyfried NT, Dammer EB, Swarup V, Nandakumar D, Duong DM, Yin L, Deng Q, Nguyen T, Hales CM, Wingo T, et al. 2017. A multi-network approach identifies protein-specific co-expression in asymptomatic and symptomatic Alzheimer's disease. *Cell Syst*. 4: 60–72.

Shionoya T. 1927. Studies in experimental extracorporeal thrombosis: V. influence of certain chemical substances on extracorporeal thrombosis with special reference to the efficacy of a combination of heparin and magnesium Sulfate. *J Exp Med*. 46:963–977.

Simic G, Babic M, Borovecki F, Hof PR. 2014. Early failure of the default-mode network and the pathogenesis of Alzheimer's disease. *CNS Neurosci Ther*. 20:692–698.

Sun Y, Lin J, Zhang L. 2019. The application of weighted gene co-expression network analysis in identifying key modules and hub genes associated with disease status in Alzheimer's disease. *Ann Transl Med*. 7:800.

Szklarczyk D, Gable AL, Lyon D, Junge A, Wyder S, Huerta-Cepas J, Simonovic M, Doncheva NT, Morris JH, Bork P, et al. 2019. STRING v11: protein-protein association networks with increased coverage, supporting functional discovery in genome-wide experimental datasets. *Nucleic Acids Res*. 47:D607–D613.

Szklarczyk D, Gable AL, Nastou KC, Lyon D, Kirsch R, Pyysalo S, Doncheva NT, Legeay M, Fang T, Bork P, et al. 2021. The STRING database in 2021: customizable protein-protein networks, and functional characterization of user-uploaded gene/measurement sets. *Nucleic Acids Res*. 49:D605–D612.

Talbot K, Wang HY, Kazi H, Han LY, Bakshi KP, Stucky A, Fuino RL, Kawaguchi KR, Samoyedny AJ, Wilson RS, et al. 2012. Demonstrated brain insulin resistance in Alzheimer's disease patients is associated with IGF-1 resistance, IRS-1 dysregulation, and cognitive decline. *J Clin Invest*. 122:1316–1338.

Tang R, Liu H. 2019. Identification of temporal characteristic networks of peripheral blood changes in Alzheimer's disease based on weighted gene co-expression network analysis. *Front Aging Neurosci*. 11:83.

Tao Y, Han Y, Yu L, Wang Q, Leng SX, Zhang H. 2020. The predicted key molecules, functions, and pathways that bridge mild cognitive impairment (MCI) and Alzheimer's disease (AD). *Front Neurol*. 11:233.

Tedde A, Piaceri I, Bagnoli S, Lucenteforte E, Ueberham U, Arendt T, Sorbi S, Nacmias B. 2011. Association study of genetic variants in CDKN2A/CDKN2B genes/loci with late-onset Alzheimer's disease. *Int J Alzheimers Dis*. 2011:374631.

Teng MH, Bartholomew JC, Bissell MJ. 1976. Insulin effect on the cell cycle: analysis of the kinetics of growth parameters in confluent chick cells. *Proc Natl Acad Sci U S A*. 73:3173–3177.

Vincent I, Rosado M, Davies P. 1996. Mitotic mechanisms in Alzheimer's disease? *J Cell Biol*. 132:413–425.

Wahl SM, Feldman GM, McCarthy JB. 1996. Regulation of leukocyte adhesion and signaling in inflammation and disease. *J Leukoc Biol*. 59:789–796.

Wang Y, Zhang X, Duan M, Zhang C, Wang K, Feng L, Song L, Wu S, Chen X. 2021. Identification of potential biomarkers associated with acute myocardial infarction by weighted gene coexpression network analysis. *Oxidative Med Cell Longev*. 2021:5553811.

Weinberg RB, Mufson EJ, Counts SE. 2015. Evidence for a neuroprotective microRNA pathway in amnestic mild cognitive impairment. *Front Neurosci*. 9:430.

Williams C, Mehrian Shai R, Wu Y, Hsu YH, Sitzer T, Spann B, McCleary C, Mo Y, Miller CA. 2009. Transcriptome analysis of synaptoneurosomes identifies neuroplasticity genes overexpressed in incipient Alzheimer's disease. *PLoS One*. 4:e4936.

Xiang X, Wind K, Wiedemann T, Blume T, Shi Y, Briel N, Beyer L, Biechele G, Eckenweber F, Zatcepin A, et al. 2021. Microglial activation states drive glucose uptake and FDG-PET alterations in neurodegenerative diseases. *Sci Transl Med*. 13:eabe5640.

Yogalingam G, Weber B, Meehan J, Rogers J, Hopwood JJ. 2000. Mucopolysaccharidosis type IIIB: characterisation and expression of wild-type and mutant recombinant alpha-N-acetylglucosaminidase and relationship with sanfilippo phenotype in an attenuated patient. *Biochim Biophys Acta*. 1502: 415–425.

Zhang T, Liu N, Wei W, Zhang Z, Li H. 2021. Integrated analysis of weighted gene coexpression network analysis identifying six genes as novel biomarkers for Alzheimer's disease. *Oxidative Med Cell Longev*. 2021:9918498.

Zhang T, Shen Y, Guo Y, Yao J. 2021. Identification of key transcriptome biomarkers based on a vital gene module associated with pathological changes in Alzheimer's disease. *Aging*. 13: 14940–14967.

Zhou Z, Bai J, Zhong S, Zhang R, Kang K, Zhang X, Xu Y, Zhao C, Zhao M. 2021. Integrative functional genomic analysis of molecular signatures and mechanistic pathways in the cell cycle underlying Alzheimer's disease. *Oxidative Med Cell Longev*. 2021:5552623.

Zuchner S, Gilbert JR, Martin ER, Leon-Guerrero CR, Xu PT, Browning C, Bronson PG, Whitehead P, Schmechel DE, Haines JL, et al. 2008. Linkage and association study of late-onset Alzheimer disease families linked to 9p21.3. *Ann Hum Genet*. 72:725–731.